2015 American Control Conference
Palmer House Hilton
July 1-3, 2015. Chicago, IL, USA

An Inversion-free Model Predictive Control with Error Compensation for Piezoelectric Actuators

Weichuan Liu, Long Cheng, Zeng-Guang Hou, Min Tan

Abstract— **This paper addresses an inversion-free model predictive control with error compensation for piezoelectric actuators (PEAs), which is based on a dynamic linearized multi-layer feedforward neural network model. By the proposed method, the inverse model of the inherent hysteresis in PEAs is not required, and the control law can be obtained in an explicit form. By using the technique of constrained quadratic programming, the proposed method still works well when dealing with the plant physical constraints. Moreover, an error compensation term is introduced into the control law to attenuate the steady-state error. To verify the effectiveness of the proposed method, experiments are conducted on a commercial PEA. The experiment results show that the proposed method has a good tracking performance for PEAs.**

Index Terms— **hysteresis, neural network modeling, dynamic linearization, model predictive control, piezoelectric actuators.**

I. Introduction

NANO-technology has been widely adopted in the high-precision positioning applications. Due to the fast response and high stiffness properties, piezoelectric actuators are becoming the core components of many high-precision systems, such as the atomic force microscope [1], computer component [2], and adaptive optics [3]. However, the inherent hysteresis nonlinearity dramatically degrades the tracking performance of PEAs under conventional control methods. Furthermore, the hysteresis nonlinearity of PEAs is also affected by the changing rate of the input voltage of PEAs (called *rate-dependent* property), which increases the difficulty of designing a desired controller. Therefore, how to overcome these difficulties has become a challenging and attractive topic in the literature.

Recently, the inversion-based method is widely adopted in the field of tracking control of PEAs. This kind of method is based on a common model structure which is composed of a linear dynamics submodel and the hysteresis submodel [4]. Under this structure, the hysteresis submodel is independent of the changing rate of input voltage, and the *rate-dependent* property is reflected by the linear dynamics submodel [5]. Therefore, the hysteresis submodel can be compensated by its inversion. To this end, the model of the hysteresis should be obtained first, and it is usually expressed by the Preisach model [6], the Prandtl-Ishlinskii model [7], the Duhem model [8] in the literature. Then the inverse hysteresis model can be calculated accordingly either by an explicit formula or in a recursive way. Once the hysteresis submodel is compensated, the only thing left is how to deal with the linear dynamics submodel, which has been well discussed in the literature [9]-[11]. However, the tracking performance of PEAs is highly dependent of the accuracy of the inverse hysteresis submodel. To alleviate this dependence, the iterative learning control (ILC) is introduced in the inversion-based method, which results in the inversion-based iterative control [12]. Here the ILC method can decrease the error between the desired trajectory and the actual displacement of PEAs, although the convergence proof of the inversion-based ILC is based on the assumption that the hysteresis submodel of PEAs is rate-independent.

To overcome the disadvantage of the inversion-based method, the inversion-free approach is drawing attention in recent years. The widely used inversion-free method is the sliding mode control (SMC). The main purpose of SMC is to guarantee the tracking performance of PEAs under the bounded disturbance and uncertainties, and the hysteresis is usually considered as a disturbance. Most of SMC schemes need the feedback of their states [14], therefore, the state observer is required [15]. Besides, chattering is an inherent problem of SMC schemes, which can greatly deteriorate the tracking performance of PEAs. To avoid the design of the state observer, an input-output-based digital SMC method is proposed in [16]. However, the chattering problem has to be solved by using boundary layer technique, which may cause the steady-state error. Some other studies are focused on the direct analysis of systems with hysteresis [17]-[18]. These results only give some theoretical discussion and are seldomly used in the real-time control of PEAs.

Model predictive control (MPC) is a promising method for tracking control of PEAs, which is suitable for the control processes with constraints [19]. In [20], an inversion-based MPC method is studied for the tracking control of PEAs. Since the inverse model of the hysteresis is needed, the disadvantage of the inversion-based method still exists. In our previous study [21], a nonlinear MPC method is proposed and realized on a commercial PEA. Although it is an inversion-free method, the control law should be obtained by solving a complicated nonlinear optimization problem, and the physical constraints of PEAs are hardly solved.

This paper proposes an inversion-free MPC with error compensation. The inverse model of hysteresis is not needed. Compared to the SMC based methods, the state observer is not required and the chattering problem can be avoided.

This work was supported in part by the National Natural Science Foundation of China (Grants 61422310, 61370032, 61225017, 61421004) and Beijing Nova Program (Grant Z121101002512066).

The authors are with the State Key laboratory of Management and Control for Complex Systems, Institute of Automation, Chinese Academy of Sciences, Beijing 100190, China. Email: long.cheng@ia.ac.cn.

The multi-layer feedforward neural network (MFNN) is introduced to approximate the behavior of PEAs, and the dynamic linearization is employed to linearize the MFNN model in each sampling interval. This dynamic linearized MFNN based model leads to an explicit control law. To decrease the steady-state error, an error compensation term is added in the control law.

II. A Multi-Layer Feedforward Neural Network Based Model of PEAs: Modeling and Dynamic Linearization

The hysteresis is a kind of memory effect, which is relied on the past input and output signals [26]. Therefore, the "nonlinear auto-regressive moving average with exogenous inputs" (NARMAX) structure is a proper way to approximate the hysteresis nonlinearity. The NARMAX model of PEAs is given as follows:

$$y(t) = \mathscr{F}(\varphi(t)), \tag{1}$$

where $\varphi(t) = [y(t-1), \cdots, y(t-n_a), u(t), \cdots, u(t-n_b)]$, $y(t)$ and $u(t)$ are the displacement and input voltage of PEAs, respectively; integers n_a and n_b are the corresponding maximum lags for $y(t)$ and $u(t)$. In this paper, a multi-layer feedforward neural network is used to approximate the nonlinear function $\mathscr{F}(\cdot)$. Since the input of $\mathscr{F}(\cdot)$ includes $u(t), \cdots, u(t-n_b)$, it can be assumed that the $\mathscr{F}(\cdot)$ includes the terms like $\big(u(t)-u(t-1)\big), \big(u(t-1)-u(t-2)\big), \cdots, \big(u(t+1-n_b)-u(t-n_b)\big)$. Therefore, the *rate-dependent* property is inherently implemental in $\mathscr{F}(\cdot)$.

A. MFNN Based Modeling of PEAs

The MFNN is set to have three layers: the input layer, the hidden layer, and the output layer. For the neurons in the hidden layer, the tangent sigmoid function is chosen as the activation function. Meanwhile, the linear unit function is chosen as the activation function in the input and output layers. The input-output relationship of MFNN can be written as follows:

$$y(t) = \sum_{j=1}^{n} w_j^o \sigma\Big(\sum_{i=1}^{m} w_{ji}^h \varphi_i(t) + w_{j0}^h\Big) + w_0^o, \tag{2}$$

where $m = n_a + n_b + 1$ is the number of neurons in the input layer, and n is the numbers of neuron in the hidden layer. The inputs of this MFNN, $\varphi_i(t)(i = 1, \cdots, m)$, are the elements of $\varphi(t)$. $\sigma(\cdot)$ denotes the tangent sigmoid function. The structure of MFNN is shown in Fig. 1. For convenience, (2) can be written in a compact form,

$$y(t) = W^o \overline{\sigma}(W^h \varphi(t)), \tag{3}$$

where $W^h \in \Re^{n\times(m+1)}$, $W^o \in \Re^{1\times(n+1)}$ are the weight matrices of the hidden layer and the output layer, respectively; $\overline{\sigma}(W^h\varphi(t)) = [1, \sigma(W_{r_1}^h\varphi), \sigma(W_{r_2}^h\varphi), \cdots, \sigma(W_{r_n}^h\varphi)]^T \in \Re^{n+1}$ ($W_{r_i}^h$ represents the ith row of matrix W^h).

The Levenberg-Marquardt (LM) training method [27] can be used to obtain the optimal W^h and W^o in an off-line way. For convenience, it is set that $W = [W^o, W_{r_1}^h, \cdots, W_{r_n}^h]^T \in \Re^{\big(n\times(m+1)+1\times(n+1)\big)\times 1}$ as the weight vector form of the weight matrices for training, then the derivative information could be obtained directly.

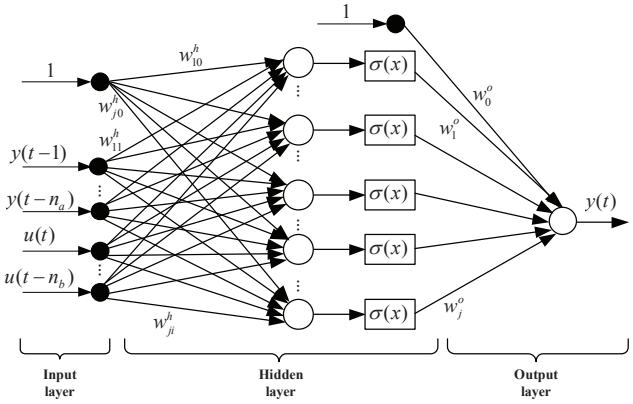

Fig. 1. MFNN model structure for PEAs.

B. Dynamic Linearization of the MFNN Based Model

At the current operating point, the dynamic linearization is carried out to extract the linearized model from the MFNN based model in each sampling interval. Since the linearized model is only used around the current operating point, it can approximate the behavior of PEAs more efficiently. Let the current operating point be $\varphi(\tau)$, then the dynamic linearized MFNN based model is expressed by Taylor-expansion:

$$\begin{aligned} y(t) - y(\tau) = &-a_1(y(t-1) - y(\tau-1)) \cdots \\ &-a_{n_a}(y(t-n_a) - y(\tau-n_a)) \\ &+b_0(u(t) - u(\tau)) \cdots \\ &+b_{n_b}(u(t-n_b) - u(\tau-n_b)), \end{aligned} \tag{4}$$

where

$a_i = -\dfrac{\partial \mathscr{F}(\varphi(t))}{\partial \varphi_i(t)}\Big|_{\varphi(t)=\varphi(\tau)}, i = (1, \cdots, n_a),$

$b_{i'} = -\dfrac{\partial \mathscr{F}(\varphi(t))}{\partial \varphi_{i'+i}(t)}\Big|_{\varphi(t)=\varphi(\tau)}, i = n_a + 1,\ i' = 0, \cdots, n_b.$

Define a bias term $\zeta(\tau) = y(\tau) + a_1 y(\tau - 1), + \cdots, + a_{n_a} y(\tau - n_a) - b_0 u(\tau), - \cdots, - b_{n_b} u(\tau - n_b)$, then equation (4) can be rewritten as

$$\begin{aligned} y(t) = &-a_1 y(t-1) \cdots - a_{n_a} y(t-n_a) \\ &+b_0 u(t) \cdots + b_{n_b} u(t-n_b) + \zeta(\tau). \end{aligned} \tag{5}$$

This dynamic linearized MFNN based model is a linear model plus a constant bias $\zeta(\tau)$, which can be considered as the influence of the hysteresis nonlinearity and the disturbance of PEAs. According to (2), the partial derivative terms defined in (4) can be calculated as follows:

$$\frac{\partial y(t)}{\partial \varphi_i(t)} = \sum_{j=1}^{n} w_j^o w_{ji}^h \big(1 - \sigma^2(\sum_{i=1}^{m} w_{ji}^h \varphi_i(t) + w_{j0}^h)\big). \tag{6}$$

III. Inversion-free MPC with error compensation

The control schematic diagram of the inversion-free MPC is shown in Fig. 2. In each sampling interval, the dynamic

linearized MFNN based model is obtained according to the current operating point, then the inversion-free MPC is designed for the tracking control of PEAs.

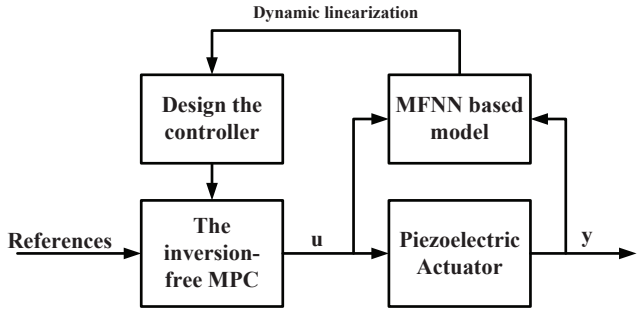

Fig. 2. Schematic diagram of the inversion-free MPC.

A. Design of the Inversion-Free MPC

The dynamic linearized MFNN based model is used as the displacement predictor. Due to the bias term $\zeta(\tau)$ is a constant during one sampling interval, the adjacent differential form of the model (5) can be employed to eliminate the bias term $\zeta(\tau)$, leading to the displacement predictor as follows:

$$\begin{aligned}\hat{y}(t+j) =&(1-a_1)\hat{y}(t+j-1)+(a_1-a_2)\hat{y}(t+j-2)\\ &\cdots+a_{n_a}\hat{y}(t+j-n_a-1)\\ &+b_0\Delta u(t+j)\cdots+b_{n_b}\Delta u(t+j-n_b),\end{aligned} \tag{7}$$

where $\hat{y}(t)$ is the predicted value of the displacement of PEAs. From the first step to the N_y-th step, the displacement predictor can be written as

$$\begin{aligned}\begin{bmatrix}\hat{y}(t+1)\\ \hat{y}(t+2)\\ \vdots\\ \hat{y}(t+N_y)\end{bmatrix} =&G\begin{bmatrix}\Delta u(t+1)\\ \Delta u(t+2)\\ \vdots\\ \Delta u(t+N_y)\end{bmatrix}\\ &+H\begin{bmatrix}\Delta u(t)\\ \Delta u(t-1)\\ \vdots\\ \Delta u(t-n_b+1)\end{bmatrix}+S\begin{bmatrix}y(t)\\ y(t-1)\\ \vdots\\ y(t-n_a)\end{bmatrix},\end{aligned} \tag{8}$$

where $G\in\Re^{N_y\times N_y}$, $H\in\Re^{N_y\times n_b}$, and $S\in\Re^{N_y\times(n_a+1)}$ are constant matrices, and this equation can be rewritten in a compact form for convenience:

$$\hat{Y}(t)=G\Delta U(t)+H\Delta U'(t)+SY'(t). \tag{9}$$

After obtaining the displacement predictor, a performance index should be designed to obtain the control law of inversion-free MPC. The performance index is defined by

$$J=[R(t)-\hat{Y}(t)]^T[R(t)-\hat{Y}(t)]+\rho\Delta U^T(t)\Delta U(t), \tag{10}$$

where $R(t)=[r(t),\cdots,r(t+N_y)]^T$ denotes the reference signal of PEAs' displacement. Parameter $\rho>0$ is a penalty term to limit $\Delta U(t)$. If constraints of inputs are not considered, the optimal control law can be obtained by solving the following equation. Since problem defined by (10) is a convex quadratic programming problem.

$$\frac{\partial J}{\partial\Delta U(t)}=0. \tag{11}$$

This results in

$$\Delta U(t)=(G^TG+\rho I)^{-1}G^T(R(t)-H\Delta U'(t)-SY'(t)). \tag{12}$$

The first element of $\Delta U(t)$ is used as the control increment for the next sampling interval. Therefore, the control signal $u(t+1)$ is given by

$$u(t+1)=u(t)+\Delta u(t+1). \tag{13}$$

It can be seen that the inversion-free MPC has an explicit form in each sampling interval. This advantage can produce a better adaptation in high-frequency tracking control of PEAs.

If constraints are considered, the optimal control law is obtained by solving a constrained optimization problem. Define the changing rate constraint and amplitude constraint as follows

$$\begin{aligned}\underline{u}\le\Delta u(t)\le\overline{u},\\ \underline{U}\le u(t)\le\overline{U}.\end{aligned} \tag{14}$$

For $\Delta U(t)$ and $U(t)=[u(t+1),\cdots,u(t+N_y)]$, the relevant constraints can be written in a matrix form:

$$C\Delta U(t)\le Q, \tag{15}$$

where

$$C=\begin{bmatrix}I_{N_y\times N_y}\\ -I_{N_y\times N_y}\\ T\\ -T\end{bmatrix},Q=\begin{bmatrix}L\underline{u}\\ -L\underline{u}\\ L\overline{U}-Lu(t)\\ -L\overline{U}+Lu(t)\end{bmatrix},$$

T is a lower triangular matrix whose non zero entries are constant one, and L is an $N_y\times 1$ vector formed by constant one.

Seeking the optimal control law of (10) subject to the constraints (15) is a constrained quadratic optimization problem. And it is solved by the active set method proposed in [28].

B. Inversion-Free MPC with Error Compensation

By (12), the optimal control law is similar to a proportional feedback closed-loop controller. Therefore, the steady-state error may occur under varied references. In order to decrease the steady-state error, an error compensation term is adopted in the control law (12), which results in the inversion-free MPC with error compensation.

Since only the first term of (12) is used for the controller design, the real controller can be rewritten as follows:

$$\begin{aligned}\Delta u(t+1)=&K_G\begin{bmatrix}1\\ z\\ \vdots\\ z^{N_y}\end{bmatrix}r(t)\\ &-K_GH\begin{bmatrix}1\\ z^{-1}\\ \vdots\\ z^{-n_b+1}\end{bmatrix}\Delta u(t)-K_GS\begin{bmatrix}1\\ z^{-1}\\ \vdots\\ z^{-n_a}\end{bmatrix}y(t),\end{aligned} \tag{16}$$

where K_G is the first row of $(G^TG+\rho I)^{-1}G^T$, and z is the forward shift operator. Define

$$K_r(z)=K_G\begin{bmatrix}1\\ z\\ \vdots\\ z^{N_y}\end{bmatrix},\ K_u(z)=-K_GH\begin{bmatrix}1\\ z^{-1}\\ \vdots\\ z^{-n_b+1}\end{bmatrix},$$

and $K_y(z)=-K_GS\begin{bmatrix}1\\ z^{-1}\\ \vdots\\ z^{-n_a}\end{bmatrix}$.

Then substituting these terms into (16) yields

$$\Delta u(t+1)=K_r(z)r(t)-K_u(z)\Delta u(t)-K_y(z)y(t). \tag{17}$$

Substituting (13) into (17) leads to

$$(1+K_u(z)z^{-1})(z-1)u(t)=K_r(z)r(t)-K_y(z)y(t). \tag{18}$$

To compensate the steady-state error, an error compensation term is added into (18). The definition of the error compensation term is

$$u_e(t)=u_e(t-1)+K_e(r(t)-y(t)). \tag{19}$$

Then the final control law is

$$\Delta u(t)=\frac{K_y(z)}{(1+K_u(z)z^{-1})(z-1)}\left(\frac{K_r(z)}{K_y(z)}r(t)-y(t)+u_e(t)\right). \tag{20}$$

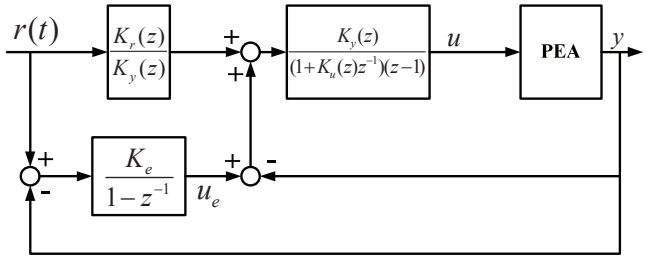

Fig. 3. Schematic diagram of the inversion-free MPC with error compensation.

The block diagram of the controller defined by (20) is illustrated in Fig. 3. It can be seen that the error compensation term affects the close-loop control system as an integrator. By the knowledge of classical control theory, the integral term has the ability to alleviate the steady-state error.

IV. Experiments and Discussions

The proposed model and control scheme are verified on a commercial PEA product (P-753.1CD, Physik Instrumente, Karlsruhe, Germany). A horizontal movement up to 15 μm can be performed by this PEA. The displacement can be measured by a built-in capacitive displacement sensor. The host computer and the amplifier of this PEA are wired to an I/O data acquisition board. The sampling time in the following experiments is set to be 0.05 ms, and the proposed model and control scheme are implemented in MATLAB/SIMULINK.

A. Verification of the MFNN based Model and the Dynamic Linearization

The identification of the MFNN based model needs to be accomplished first. According to [29], the structure of the MFNN based model of PEAs could be chosen as a second-order system, *i.e.*, $n_a=2$. Meanwhile, n is chosen to be 5. n_b is set to be 1. A mixed sinusoid voltage $u_d(t)$ is used to excite the PEA. The amplitude of this voltage input is from 0 V to 80 V, while the frequency is between 1 Hz to 400 Hz. Then the displacement of the PEA, $y_d(t)$, is measured under this mixed sinusoid vlotage input. With the training data set $[u_d(t),y_d(t)]^T$ and the weight vector W, the MFNN based model can be obtained by the LM training method.

Figure 4 gives the experiment results of the MFNN based model. The output of the MFNN based model is close to the real displacment of PEAs. This means that the MFNN based model has a good performance to approximate the dynamical behavior of PEAs. Furthermore, the behavior of PEAs is dramatically different with the increase of the sinusoid voltage's frequency. Notably, the MFNN based model also has a good match, which means that it has the *rate-dependent* property.

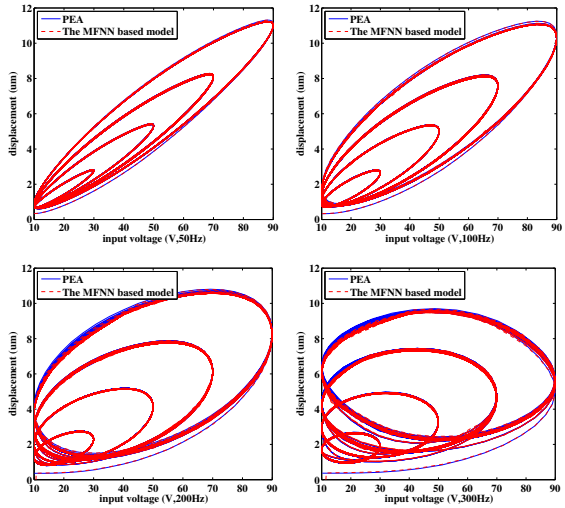

Fig. 4. The displacements of the PEA and MFNN based model under different sinusoid input voltages.

B. Verification of the Inversion-Free MPC with Error Compensation

Comparison experiments of the inversion-free MPC with and without error compensation are also conducted on the PEA. The parameter ρ is set to be 30 and $K_e=0.01$. The experiment result is given in Fig. 5. It can be seen that the inversion-free MPC with error compensation has a better tracking performance compared with the inversion-free MPC without error compensation. The experiment results suggest that the error compensation term could effectively decrease the steady-state error, resulting in a better tracking performance.

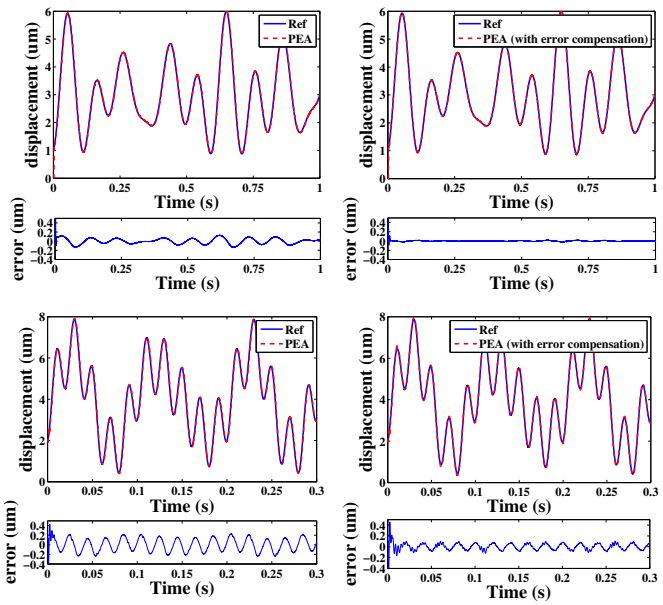

Fig. 5. Compared experiments of the inversion-free MPC with and without error compensation.

The tracking performance of the inversion-free MPC with error compensation for high frequency references are given in Fig. 6. Sinusoid references with 200 Hz and 300 Hz are adopted as the desired trajectory. The experiment results suggest that the tracking performance of the inversion-free MPC with error compensation is satisfactory.

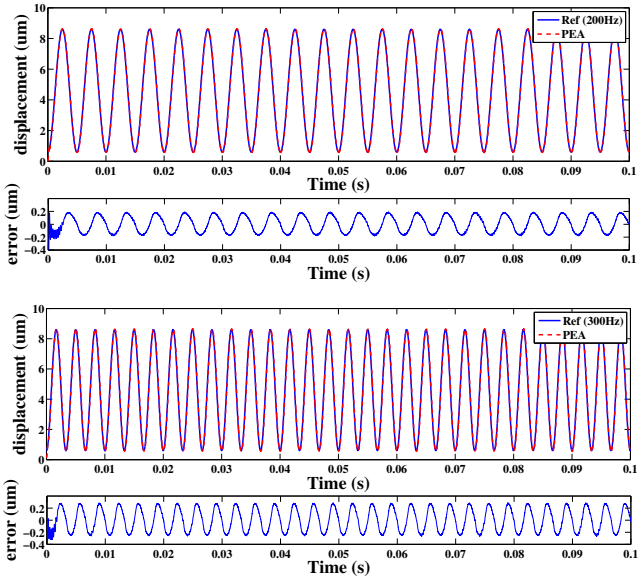

Fig. 6. Tracking performance of the inversion-free MPC with error compensation under high frequency references.

To compare the tracking performance of the SMC method and the inversion-based method, the PID-based SMC scheme proposed in [13] and the inversion-based MPC approach proposed in [20] are both used in the experiments. For the PID-based SMC scheme, the reference is defined as $r(t) = 5sin(2\pi ft - \frac{\pi}{2}) + 5$, f is the frequency of the signal. The root mean square (RMS) value of the error between the desired trajectory and the displacement of the PEA is used as the performance index. Meanwhile, a special reference signal SW defined in [20] is introduced in the experiments. The definition of SW is set as $SW = 0.5\big(\frac{30}{7}sin[\frac{2\pi f_{max}}{20}(t-0.1)+\pi] + \frac{25}{7}sin[\frac{2\pi f_{max}}{5}(t-0.1)+0.5\pi] + \frac{5}{7}sin[\frac{2\pi f_{max}}{2}(t-0.1)+0.2\pi] + \frac{5}{7}sin[2\pi f_{max}(t-0.1)]\big) + 5$, where f_{max} is the maximum frequency.

The comparison experiments results are listed in Table I. Compare with the PID-based SMC scheme, the inversion-free MPC with error compensation has a better tracking performance than the PID-based SMC scheme, especially in the high frequency reference case. Compared with the inversion-based method, the tracking accuracy has an notable improvement by the inversion-free MPC with error compensation under the low frequency case.

TABLE I

THE COMPARISON EXPERIMENTS BETWEEN THE PROPOSED METHOD AND THE APPROACH IN [13] OR [20]. THE ROOT MEAN SQUARE (RMS) ERROR OF THE DISPLACEMENT ERROR VECTORS ARE LISTED.

	References	the proposed method	the method in [13] or [20]
Sinusoid references from [13]	$f = 1$ Hz	0.0054 μm	0.008 μm
	$f = 5$ Hz	0.0079 μm	0.012 μm
	$f = 10$ Hz	0.0178 μm	0.018 μm
	$f = 50$ Hz	0.0489 μm	0.051 μm
	$f = 100$ Hz	0.0773 μm	0.086 μm
	$f = 150$ Hz	0.1166 μm	0.138 μm
SW from [20]	f_{max}=10Hz	0.0014 μm	0.009 μm
	f_{max}=50Hz	0.0237 μm	0.025 μm

C. Comparison of Control with Constraints

Besides the tracking performance, constraints on the input voltage of PEAs is another vital factor in industrial applications. Although it increases the computational burden to obtain the optimal control law, a better transient response has been reported in some situations.

The comparison experiments of the inversion-free MPC with constraints and the hard limiting method (the hard limiting method means that the input voltage of PEAs will maintain its upper/lower bound values if the calculated input voltage exceeds the physical limit) are given in Fig. 7: the transient trajectory of the step response of the PEA and the variation of the input voltage. In this experiment, it is set that $\rho = 80$ and $K_e = 0$. The limits of $u(t)$ in (15) are given as: $\underline{u} = -5$, $\overline{u} = 5$, $\underline{U} = -65$, and $\overline{U} = 65$.

It can be seen that the overshoot of the inversion-free MPC with constraints is less than the one based on the hard limiting method. This suggests that the constrained inversion-free MPC can reach the reference faster than the one based on the hard limiting method.

V. Conclusions and Future Works

An inversion-free MPC with error compensation is proposed in this paper. First, the dynamic linearization is intro-

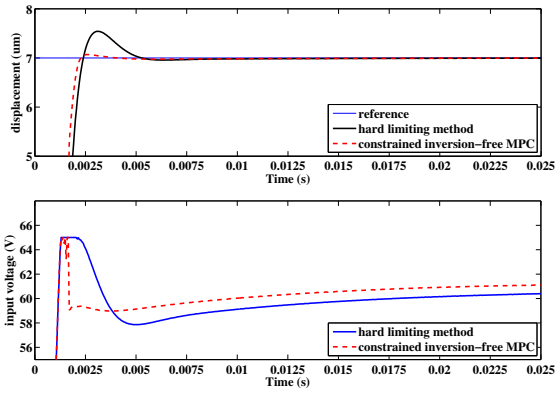

Fig. 7. Comparison experiments of the inversion-free MPC with and without constraints.

duced to linearize the MFNN based model, which results in the dynamic linearized MFNN based model. This dynamic linearized MFNN based model leads to the optimal control law in an explicit form. After that, the constraints on the inputs of PEAs are considered. Furthermore, the steady-state error is compensated by an error compensation term, resulting in the inversion-free MPC with error compensation. To verify the proposed model and control scheme, experiments are conducted on a PEA. Comparison experiments illustrate the effectiveness of the proposed method.

In this paper, only the constraints on the inputs of PEAs are considered. If the constraints on the outputs of PEAs can also be handled, the proposed constrained MPC approach in this paper will be more practical. When these constraints are considered, the constrained optimization problem will become more complex. Therefore, to ensure the computational speed of the constrained MPC approach, the methods in [22]-[25] can be adopted to solve the constrained optimization problem effectively. These ideas will be studied in the future.

REFERENCES

[1] D. Croft, G. Shed and S. Devasia, "Creep, hysteresis, and vibration compensation for piezoactuators: atomic force microscopy application," *ASME Journal of Dynamic Systems, Measurement, and Control*, vol. 123, no. 1, pp. 35-43, May. 2001.

[2] W. Yang, S. -Y. Lee, and B. -J. You, "A piezoelectric actuator with a motion-decoupling amplifier for optical disk drives," *Smart Materials and Structures*, vol. 19, no. 6, pp. 065027.1-065027.10, May. 2010.

[3] H. Song, G. Vdovin, R. Fraanje, G. Schitter , and M. Verhaegen, "Extracting hysteresis from nonlinear measurement of wavefront-sensorless adaptive optics system," *Optics Letters*, vol. 34, no. 1, pp. 61-63, May 2009.

[4] S. Devasia, E. Eleftheriou, and S. O. R. Moheimani, "A survey of control issues in nanopositioning," *IEEE Transactions on Control Systems Technology*, vol. 15, no. 5, pp. 802-823, Sep. 2007.

[5] J. Y. Peng and X. B. Chen, "A survey of modeling and control of piezoelectric actuators," *Modern Mechanical Engineering*, vol. 3, no. 1, pp. 1-20, Feb. 2013.

[6] H. Hu, and R. B. Mrad, "On the classical preisach model for hysteresis in piezoceramic actuators," *Mechatronics*, vol. 13, no. 2, pp. 85-94, Feb. 2002.

[7] K. Kuhnen, and F. Previdi, "Modeling, identification and compensation of complex hysteretic nonlinearities: a modified Prandtl-Ishlinskii approach," *European Journal of Control*, vol. 9, no. 4, pp. 407-421, 2003.

[8] Y. Cao, and X. B. Chen, "A novel discrete ARMA-based model for piezoelectric actuator hysteresis," *IEEE/ASME Transactions on Mechatronics*, vol. 17, no. 4, pp. 737-744, Aug. 2012.

[9] G. Song, J. Zhao, X. Zhou, and J. Alexis De Abreu-García, "Traching control of a piezoceramic actuator with hysteresis compensation using inverse preisach model," *IEEE/ASME Transactions on Mechatronics*, vol. 10, no. 2, pp. 198-209, Apr. 2005.

[10] C. Ru, L. Chen, B. Shao, W. Rong, and L. Sun, "A hysteresis compensation method of piezoelectric actuator: model, identification and control," *Control Engineering Practice*, vol. 17, no. 9, pp. 1107-1114, 2009.

[11] B. Mokaberi, and Aristides A. G. Requicha, "Compensation of scanner creep and hysteresis for AFM nanomanipulation," *IEEE Transactions on Automation Science and Engineering*, vol. 5, no. 2, pp. 197-206, Apr. 2008.

[12] Y. Wu, and Q. Zou, "Iterative control approach to compensate for both the hysteresis and the dynamics effects of piezo actuators," *IEEE Transactions on Control System Technology*, vol. 15, no. 5, pp. 936-944, Sep. 2007.

[13] J. Y. Peng, and X. B. Chen, "Integrated PID-based sliding mode state estimation and control for piezoelectric actuators," *IEEE/ASME Transactions on Mechatronics*, vol. 19, no. 1, pp. 88-99, Feb. 2014.

[14] C. Edwards, and S. K. Spurgeon, *Sliding Mode Control: Theory and Applications*, Abingdon, U.K., Taylor & Francis., 1998.

[15] J. C. Shen, W. Y. Jywel, C. H. Liu, Y. T. Jian, and J. Yang, "Sliding mode control of a three-degrees-of-freedom Nanopositioner," *Asian Journal of Control*, vol. 10, no. 3, pp. 267-276, 2008.

[16] Q. Xu, "Digital sliding-mode control of piezoelectric micropositioning system based on input-output Model," *IEEE/ASME Transactions on Industrial Electronics*, vol. 61, no. 10, pp. 5517-5526, 2014.

[17] S. Valadkhan, K. Morris, A. Khajepour, "Stability and robust position control of hysteretic systems," *International Journal of Robust and Nonlinear Control*, vol. 20, no. 4, pp. 460-471, 2010.

[18] A. Esbrook, X. Tan, and H. Khalil, "Inversion-free stabilization and regulation of systems with hysteresis via integral action," *Automatica*, vol. 50, no. 4, pp. 1017-1025, 2014.

[19] L. Zhang and R. D. Braatz, "On switched MPC of a class of switched linear systems with modal dwell time," in *Proceedings of the 52nd IEEE Conference on Decision and Control*, Florence, Italy, Dec. 2013, pp. 91-96.

[20] Y. Cao, L. Cheng, X. B. Chen, and J. Y. Peng, "An inversion-based model predictive control with an integral-of-error state variable for piezoelectric actuators," *IEEE/ASME Transactions on Mechatronics*, vol. 18, no. 3, pp. 895-904, Jun. 2013.

[21] W. Liu, L. Cheng, Z. -G. Hou, J. Yu, and M. Tan, "Neural network based nonlinear model predictive control for piezoelectric actuators," submitted to *IEEE Transactions on Industrial Electronics*, 2014.

[22] L. Cheng, Z. -G. Hou, and M. Tan, "Solving linear variational inequalities by projection neural network with time-varying delays," *Physics Letters A*, vol. 373, no. 20, pp. 1739-1743, 2009.

[23] L. Cheng, Z. -G. Hou, and M. Tan, "A neutral-type delayed projection neural network for solving nonlinear variational inequalities," *IEEE Transactions on Circuits and Systems II: Express Briefs*, vol. 55, no. 8, pp. 806-810, 2008.

[24] L. Cheng, Z. -G. Hou, and M. Tan, "A delayed projection neural network for solving linear variational inequalities," *IEEE Transactions on Neural Networks*, vol. 20, no. 6, pp. 915-925, 2009.

[25] L. Cheng, Z. -G. Hou, Y. Lin, M. Tan, W. J. Zhang, and F. -X. Wu, "Recurrent neural network for non-smooth convex optimization problems with application to the identification of genetic regulatory networks," *IEEE Transactions on Neural Networks*, vol. 21, no. 5, pp. 714-726, 2011.

[26] V. Hassani, T. Tjahjowidodo, and T. N. Do, "A survey on hysteresis modeling, identification and control," *Mechanical Systems and Signal Processing*, vol. 49, no. 1, pp. 209-233, 2014.

[27] M. Norgaard, O. Ravn, N. K. Poulsen, and L. K. Hansen, *Neural Networks for Modelling and Control of Dynamic Systems*, Springer-Verlag, 2000.

[28] J. M. Maciejowski, *Predictive Control: with Constraints*, Prentice Hall, 2002.

[29] X. B. Chen, Q. S. Zhang, D. Kang, and W. J. Zhang, "On the dynamics of perzoelectric positioning systems," *Review of Scientific Instruments*, vol. 79, pp. 116101-1-116101-3, Oct. 2008.